Probabilistic Nonlinear Analysis of a RC Shear Wall Structure including Soil-Structure Interaction

A. Hashemi, T. Elkhoraibi & F. Ostadan
Bechtel National Inc., San Francisco, USA

SUMMARY:
The probabilistic seismic response of a reinforced concrete (RC) shear wall building typical of nuclear industry structures is evaluated by explicit consideration of structural nonlinearity and soil-structure interaction (SSI). The analysis is carried out in three stages: (1) site response analysis, (2) soil structure interaction analysis, and (3) nonlinear structural analysis. The nonlinear analysis is part of a comprehensive Integrated Soil-Structure Fragility Analysis (ISSFA) which evaluates the annual failure probability of the building, when supported on rock or soil subgrades, as the measure of its seismic performance. The site response analysis, soil structure interaction analysis and details of the fragility analysis will be discussed in future publications. The nonlinear model development and uncertainty considerations in nonlinear modeling are discussed in this paper. A sample of the results of the probabilistic SSI analysis (a sub-analysis of ISSFA) highlighting the structural nonlinearity effects in soil and rock sites is also provided.

Keywords: Probabilistic SSI, Structural nonlinearity, Fragility Analysis, Performance based, Squat Shear walls.

1. INTRODUCTION

The nonlinear analysis described in this paper is part of a comprehensive Integrated Soil-Structure Fragility Analysis (ISSFA) which evaluates the seismic performance of a reinforced concrete (RC) shear wall building, typical of nuclear industry structures by quantifying its annual failure probability. The ISSFA methodology is described in Hashemi et al. (2009) and Elkhoraibi et al. (2011). The graphical representation of the ISSFA methodology is presented in Figure 1. The seismic response of the building is evaluated by explicit consideration of structural nonlinearity and soil-structure interaction (SSI). The structure is designed to remain elastic at 10,000 year return period seismic hazard level. The analysis is carried out in three stages: (1) site response analysis, (2) soil structure interaction analysis, and (3) nonlinear structural analysis. The site response analysis is carried out to obtain the free-field seismic ground motion and strain-compatible soil properties at the building site. The SSI analysis is performed using SASSI2010 (Bechtel, 2011), which explicitly includes the FE model of the structure as well as the subsurface in a linear frequency domain analysis and uses the free-field ground motions and strain-compatible soil profiles from stage (1) as input. Finally, the nonlinear response-history analysis is carried out in OpenSEES (Mazzoni et al., 2006) using the foundation motion from stage (2) as input and explicitly including significant structural nonlinearities. The nonlinear model development and uncertainty considerations in nonlinear modeling are discussed below. A sample of the results of the probabilistic SSI analysis (a sub-analysis of ISSFA) including the structural nonlinearity are also provided in this paper. More detailed description and discussions will be provided in future publications.

The analysis of typical nuclear structures rarely account explicitly for structural nonlinearity when subjected to their design and beyond design basis earthquake events. Commonly used methods attempt to estimate the effects of structural nonlinearity through empirical or prescribed factors. This simplified approach has the following shortcomings:

- It is a prescribed and not quantified approximation of a phenomenon which depends on the configuration, robustness, resilience, and redundancies in the lateral resisting system.
- It does not address the inelastic response of the structures at beyond design basis seismic events nor any deformation concentration in the structure due to local yielding of components.
- It does not provide any insight into the change in the probabilistic distribution of the inelastic demand.

Nevertheless, due to its simplicity, the approach is commonly used to provide an overall assessment of the structural behavior due to extreme events.

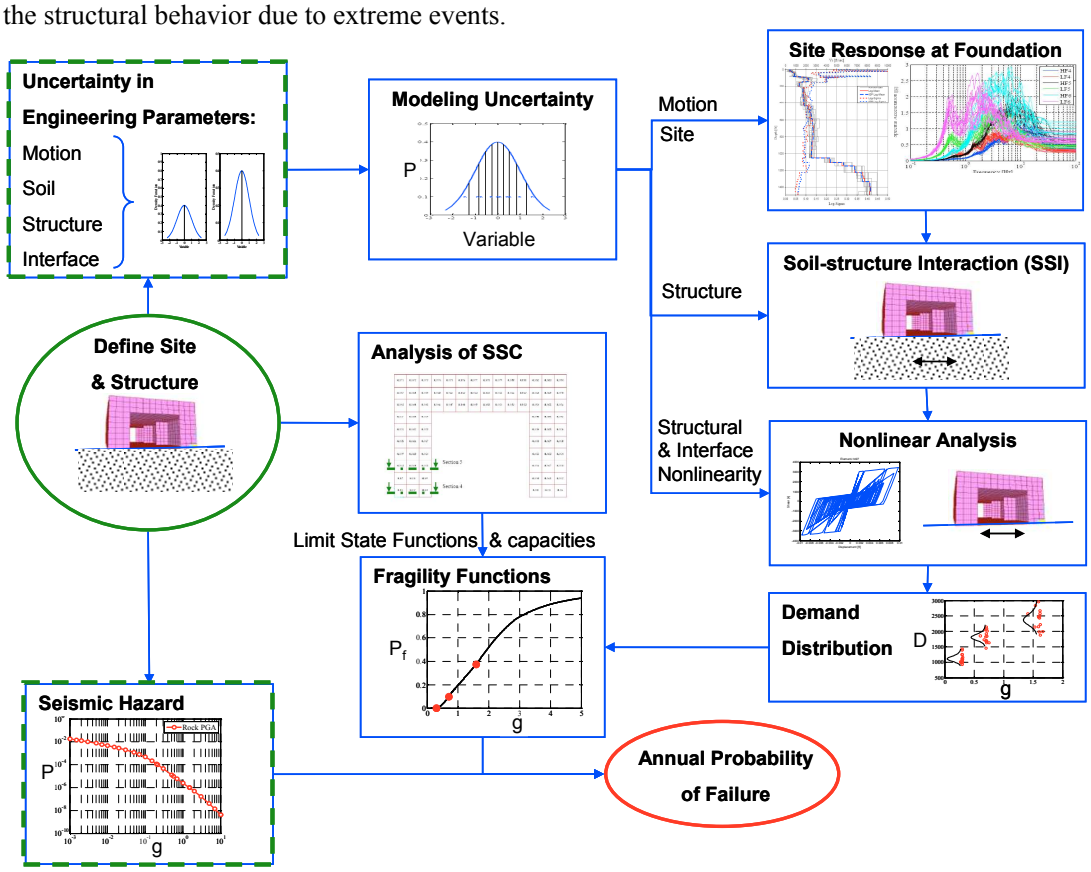

Figure 1. Integrated Soil-Structure Fragility Analysis (ISSFA) Methodology

In order to address the shortcomings listed above, this paper provides an example of explicit consideration of structural nonlinearity in the analysis of a typical nuclear structure which is governed by in-plane shear in its lateral load resisting mechanism. The subject structure for this study and its corresponding finite element (FE) representation are described in Section 2. In order to facilitate the nonlinear modeling of the structure, a simplified nonlinear model (stick model) is developed which is equivalent to the FE model in its dynamic responses. The nonlinear features which are expected to control the lateral response of the structure are added to the stick model. In this case, all shear walls in the structure are explicitly modeled by defining their backbone curves and hysteretic behavior. In order to reflect the uncertainties in the modeling parameters for the probabilistic analysis, using the Latin-Hypercube Sampling (LHS) technique (McKay et al. 1979), a set of 30 different nonlinear models is generated. The set of nonlinear models developed is used in the nonlinear response history analyses at three different hazard intensity levels (namely 1E4 year, 1E5 year and 1E6 year return periods) to calculate the distribution of important engineering demand parameters (e.g. drift ratios) at each of these levels. These demand distributions are used in fragility function calculations as part of the ISSFA methodology to estimate the annual probability of failure for the structure.

2. STRUCTURAL MODEL

The selected structure, shown in Figure 2(a) is a representative nuclear facilities building with a footprint of about 160 ft by 105 ft on a 6 ft mat foundation at El. 0 and supported by reinforced concrete walls ranging in thickness from 2 to 3 ft and the majority of slabs of 2 ft thickness with some exceptions of up to 3 ft slabs. Four major shear walls provide lateral load resistance in the long (East-West (X)) direction of the structure while three shear walls provide that resistance in the short (North-South (Y)) direction, as shown in the cross-sectional view in Figure 2(c). The structure consists of 2 main floors extending on the entire footprint at El .33 ft and El. 62 ft, and a third floor occupying the middle 63 ft of the North-South direction and the full width in the other direction at El 80 ft. Steel beams form a platform between El 46 ft and El 62 ft as shown in the middle portion of the structure in Figure 2(b). The roof elevation is at El. 114 ft. The FE model of the structure is developed using the computer program SASSI2010 using thick shell elements for the mat foundation, walls and slabs. For the purpose of nonlinear analysis, reinforcement ratios are defined for the structure based on the design-basis event demand, calculated using the deterministic SSI approach similar to that described in Hashemi et al. (2011). Story drifts are calculated in the East-West (X) and North-South (Y) directions along a vertical line passing through node 8188, shown in Figure 2(c), which is located at the intersection of shear walls. The main structural characteristics for the structure are summarized in Table 2.1. The fundamental natural frequencies of the structure and their corresponding mass participation factors (MPF) are presented in Table 2.2.

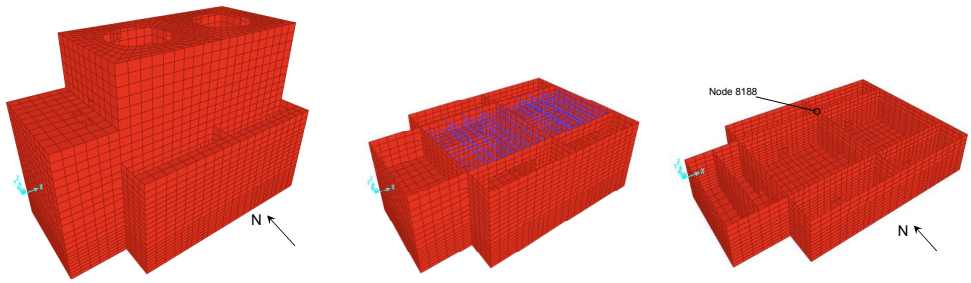

(a) 3D View (b) First Floor (EL 31.25 ft) (c) Basemat

Figure 2. Selected Structure – 3D Views

Table 2.1. Structure and Model Summary

Number of Nodes	9614
Shell Elements	5743
Beam Elements	652
Footprint	160 ft x 105 ft
Height	114 ft
Embedment Depth	19 ft
Foundation Thickness	6 ft
Slab Thickness	2 to 3 ft
Wall Thickness	2 to 3 ft
Total Weight	76800 kips
Foundation Area	15500 ft^2
Average Soil Pressure	4.95 kip/ft^2
Concrete Elastic Modulus	3950 ksi

Table 2.2. Major Fixed Base Modal Frequencies

Direction	1st Mode		2nd Mode		3rd Mode	
	Frequency	MPF	Frequency	MPF	Frequency	MPF
East-West (X)	6.0 Hz	32%	8.4 Hz	17%	10.5 Hz	8%
North-South (Y)	5.3 Hz	18%	6.3 Hz	18%	9.5 Hz	26%

3. NONLINEAR MODEL DEVELOPMENT

The shear walls in the building have height to length ratios of less than 1 (squat shear walls) and are flexurally very stiff about their major axes. Therefore, the lateral dynamic response of the subject structure is governed by the shear deformation of the walls with little contribution from bending. The analysis is carried out using OpenSEES where the nonlinear response of structural shear walls can be effectively modeled using an elastic beam representation of the walls supplemented by a nonlinear spring. For this reason, the FE model described above is converted to a more simplified model where all shear walls are represented by vertical elastic beam elements (stick model). The in-plane and out-of plane cross section properties of each stick is calculated for the cross section of their corresponding concrete wall (total of 35 sticks) in the FE model and placed at the center of rigidity of its corresponding concrete wall. Note that the FE representations of the floor concrete slabs in the FE model are not altered in the stick model. The connection between the sticks and floor concrete slab are provided by in-plane rigid beams along the length of each wall at the concrete floor location, therefore, the torsional characteristics of the FE model are maintained in the stick model. The schematic views of the FE model and the stick model of the structure are provided in Figure 3. These figures also show the major structural walls on column lines 2 (X direction) and B (Y direction), respectively.

The adequacy of the stick model is verified by comparing major natural frequencies, mass participation factors, and mode shapes of the stick model with those of the FE model as well as comparing the displacement time-history and maximum displacements at different elevations in the structure. These comparisons are documented in Elkhoraibi et al. (2012) and confirm a very good agreement between the global results of the two models with the difference limited to only 12%. Also note that in most cases the stick model is resulting in slightly more conservative displacements.

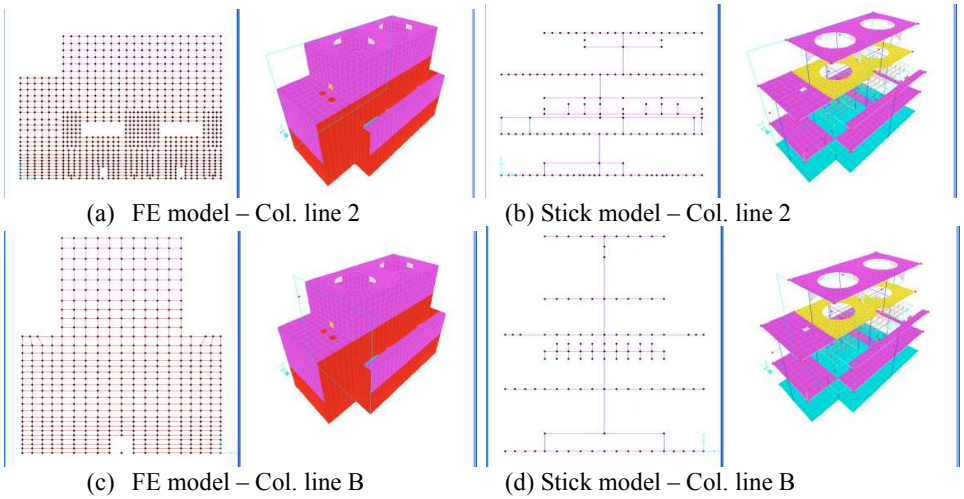

(a) FE model – Col. line 2 (b) Stick model – Col. line 2

(c) FE model – Col. line B (d) Stick model – Col. line B

Figure 3. Comparison of the FE and Stick Model

The lateral load resisting system in the structure consists of shear walls with aspect ratios of less than 1.0 in both X and Y directions. The expected structural nonlinearity in this structure is therefore, entirely due to the nonlinear in-plane shear response of the walls. The flexural response of the walls are expected (and later confirmed) to remain within the elastic range. The median strength of these walls are obtained from the capacity formulation for low-rise concrete shear walls ($\frac{h_w}{l_w} \leq 2.0$) in ASCE 43-05. Since the intent is to obtain the best estimate capacity of the wall (not a conservative estimate), strength reduction factor (ϕ) of unity is consistently used. The ASCE43-05 (2005) formulation is repeated in Eqn. 3.1 for convenience, where ϕ is the capacity reduction factor, v_u.is the ultimate shear strength, f'_c is the concrete compressive strength (psi), h_w, l_w, and t_n are the wall height, length, and thickness, respectively, N_A is the wall axial load, f_y is the steel yield strength, and ρ_{se} is defined as a

weighted average of the vertical and horizontal steel reinforcement ratio which is equal to the vertical reinforcement ratio for $\frac{h_w}{l_w} \leq 0.5$ and equal to the horizontal reinforcement ratio for $\frac{h_w}{l_w} \geq 1.5$ and linearly interpolated in between. Note that the shear wall capacity is determined as $v_u \times 0.6 l_w \times t_n$.

$$v_u = \phi \left[8.3\sqrt{f'_c} - 3.4\sqrt{f'_c}\left(\frac{h_w}{l_w} - 0.5\right) + \frac{N_A}{4 l_w t_n} + \rho_{se} f_y \right] \quad (3.1)$$

The nonlinear backbone curve for the shear response of these walls are obtained from the provisions of the ASCE41-06 (2007), Supplement-1, Chapter 6. These provisions specify a shape for the backbone curve defined by drift and strength ratio parameters as shown in Figure 4 (a), where Q and Q_y represent the strength and yield strength of the wall and Δ/h is the total drift ratio (including flexure) for the wall. Points F, B, and C on the backbone curve identify the cracking of concrete, yielding of reinforcement, and loss of strength (structural failure) of the wall. Since the axial load on the walls for the selected structure does not exceed the 5% of the $A_c f'_c$, the best estimate backbone parameters d, e, g, c and f for the walls are selected as 1.0, 2.0, 0.4, 0.2, and 0.6, respectively for all walls, refer to ASCE41-06.

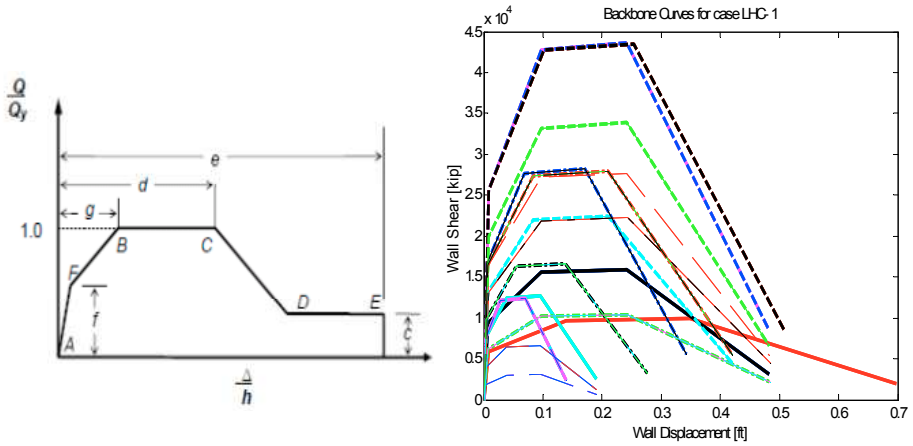

(a) Generic (ASCE 41-06, Supplement-1) (b) First Realization for all 35 walls

Figure 4. Backbone Curves for Shear Walls in the Nonlinear Stick Model

In the ISSFA analysis of the subject structure (of which, the nonlinear analysis presented here is a component), 5 parameters are identified for uncertainty modeling. These parameters are dynamic soil profile properties, young's modulus for concrete (E_C), structural damping ratio (D), shear wall modeling drift limit parameter, (d), and coefficient of friction for sliding (μ). These parameters are selected and randomly paired following Latin Hyper-cube Sampling (LHS) methodology as described in Hashemi et al. (2009). The uncertainty in the backbone curves is considered using a log-normal distribution for the drift limit parameter d with mean of 1% and standard deviation of 0.4. Values of the other drift parameters g and e are assumed to be perfectly correlated with d and taken as 0.4d and 2.0d, respectively. The uncertainty in the strength of each wall is considered through the uncertainty in E_c (thus, uncertainty in f'_c) for each wall. Therefore, the strength parameters f, and c are not further varied in the randomizations process. Through the LHS, 30 samples are generated for each one of the backbone curves for each wall. Figure 4 (b) presents the backbone curves for all 35 shear walls of the subject structure in the first realization of the LHS simulation. The randomized backbone curves for stick 26 (2nd story-X direction on line 2) and stick 20 (1st story – Y direction on line B) are presented as representative examples in Figure 5**.**

ASCE 41-06 specifies the backbone curves but does not provide any insight in cyclic response of the shear walls. Since the purpose of the nonlinear modeling here is to perform nonlinear response history

analysis (as opposed to static analysis), the proper selection of parameters controlling the cyclic response of the shear walls such as the definition of the pinching response and damage modeling is imperative. These parameters are selected by calibrating the nonlinear model with the results of cyclic tests performed by Wang, et.al. (1975) on a model of a shear wall (one-third scale) with height to length of 0.5 and height to thickness ratio of 12. The height to length ratio for the walls of the selected structure range from 0.20 to 0.96 and the height to thickness ratio for its walls range from 3.2 to 24. Figure 6 shows the experiment set up and dimensions for the shear wall cyclic tests as well as the shear wall modeling approach and backbone curve adopted for the calibration purpose. The comparison of the shear force versus shear deformation for the test results and the calibrated model are provided in Figure 7. Note that the effect of pinching and damage parameters on the nonlinear response are secondary to the backbone curve, therefore, these parameters are not varied in the LHS of the nonlinear models.

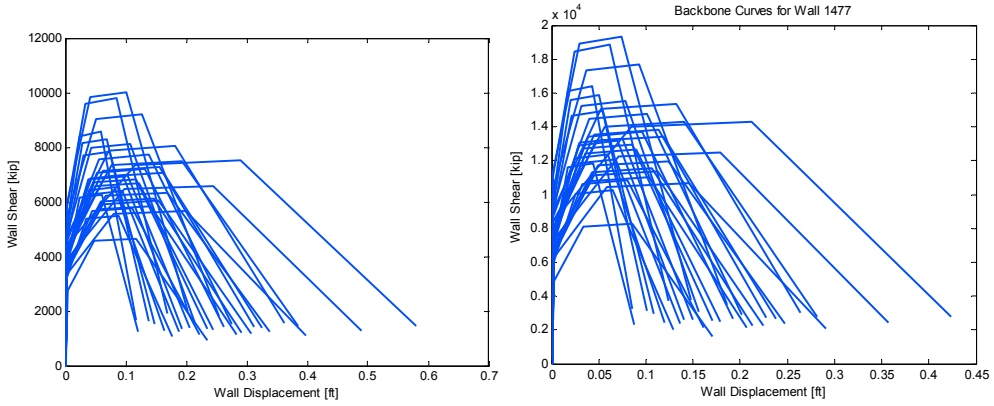

(a) Stick 26 (b) Stick 20

Figure 5. Variation of the Backbone Curved Considered in LHS for the Nonlinear Analysis

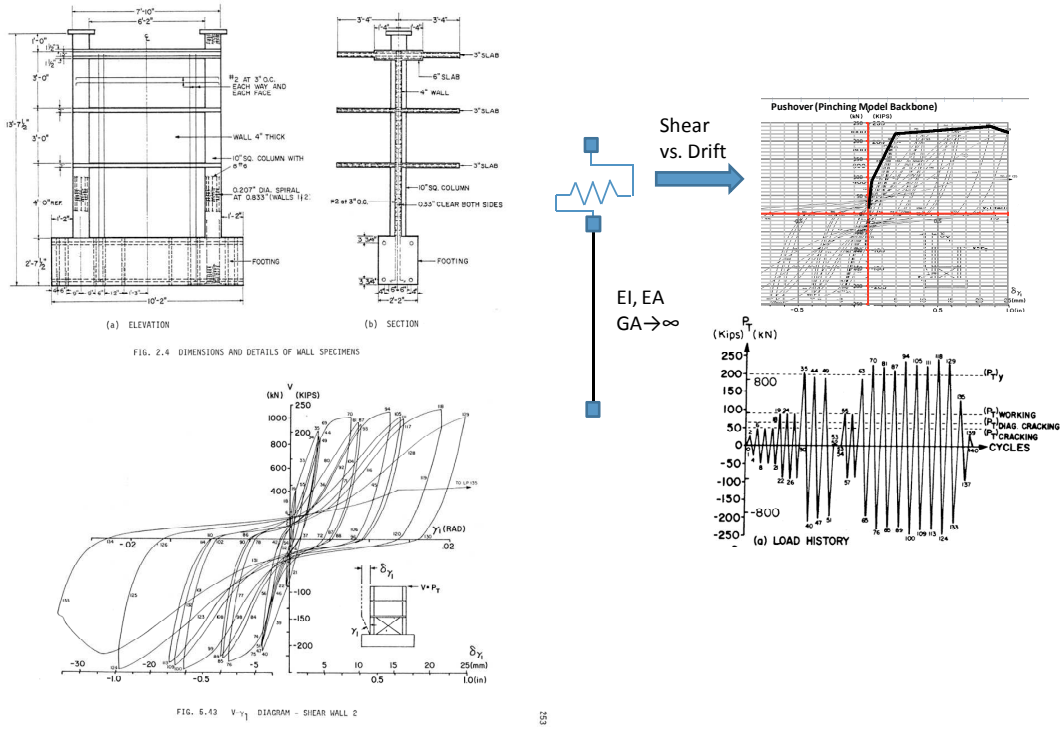

Figure 6. One-third Scale Test Specimen for Cyclic Shear Wall Tests Used in Calibration of the Cyclic Response of the Shear Walls (Wang et al. 1975)

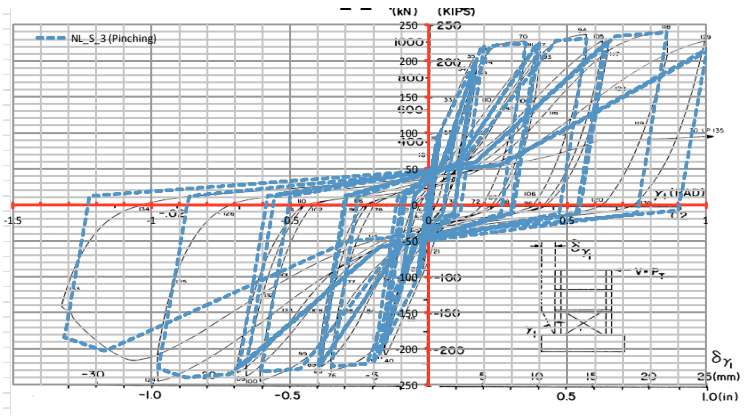

Figure 7. Nonlinear Model Calibration to the Shear Wall Experimental Cyclic Response

4. SSI ANALYSIS AND FOUNDATION MOTION DEVELOPMENT

In the ISSFA analysis of the subject structure (of which the nonlinear analysis presented here is a component), two different site conditions, namely a shallow rock subgrade and a deep soil subgrade representative of sites at the East coast of the United States, are considered. Each nonlinear response-history analysis case is performed as a fixed-base analysis, where the SSI effects are included by using a foundation motion which is different than the free field motion and is obtained from the corresponding 3D SSI analysis of the site and structure using SASSI2010. The details of the SSI analysis are not in the scope of this paper and are documented in Elkhoraibi et al. (2012). For the rock analysis the rotational components of the foundation motion are negligible and only the translational motion in X, Y, and Z directions are considered as uniform accelerations recorded on a node at the intersection of column lines 2 and B (major walls in X and Y directions, respectively) on the basemat of the structure. For the soil analysis the complete foundation motion (including foundation rotations) is applied as the foundation input displacement time-history. The nonlinear RHA applies the foundation acceleration or displacement time-histories in all directions simultaneously.

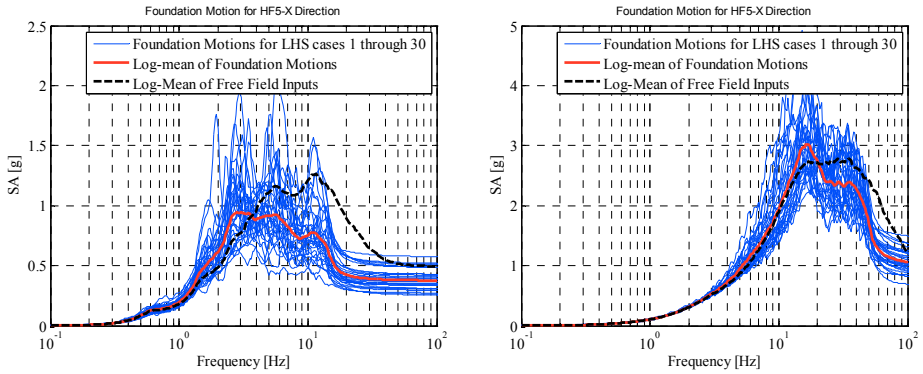

(a) Soil site (b) Rock site

Figure 8. Foundation Motion ARS for HF Motion at Intensity Level 1E-5, X Direction

The acceleration response spectra of the foundation motions obtained from the SSI analyses of the structure subjected to high frequency (HF) and low frequency (LF) motions at 1E-4, 1E-5, and 1E-6 intensity levels (return periods of 1E4, 1E5, and 1E6 years, respectively) for both soil and rock subgrades are calculated. Figure 8 (a) and (b) provide a sample of these results for HF motions (30 realizations) at 1E5 intensity level in the X direction for the soil site and the rock site, respectively. In the figures shown, the log-mean of the foundation acceleration response spectra (ARS) and the log-

mean of the free-field surface ARS are also provided for comparison. It is observed that the SSI effects for the soil site subject to a horizontal HF input motion includes a significant shift in the frequency content of the input motion to the lower frequencies and reduction in the peak of the response spectra. For the rock site the SSI effects are generally much less significant when compared to the soil site case. Nevertheless, a shift toward lower frequencies is generally observed as well as amplification at the SSI frequency of the structure on rock (around 15 Hz in this case).

5. NONLINEAR RESPONSE HISTORY ANALYSIS (RHA)

The 3D nonlinear RHA is carried on using the nonlinear model described above in OpenSEES, using the foundation motion time-histories (spectra of which for HF 1E-5 level is shown in previous section) as input. The OpenSEES analysis is a time-domain analysis using Newmark integrator (gamma = 0.5, beta = 0.25) and mass and stiffness proportional damping defined in terms of structural frequency. Note that the value of the assigned nominal damping ratio varies in each realization of the structural model (30 LHS cases) according to a lognormal distribution with mean of 5% and log-standard deviation of 0.6. The analysis time step is 0.005 sec which is reduced to 0.000625 sec if convergence is not achieved in any step. For each step the convergence test is carried on the basis of the total energy corresponding to the unbalanced forces and displacements with a threshold of 10^{-8} kip-ft.

The nonlinear RHA results are obtained for $30 \times 2 \times 3 \times 2 = 360$ runs (30 realizations for the HF and LF motions at 1E4, 1E5, and 1E6 intensity levels on soil or rock subgrades). The case selected for presentation below is the 16th realization of the HF motion, 1E6 intensity level on the rock site. This case exhibited one of the most severe nonlinear response observed in the analysis of the structure. The results presented here are for the major walls at column line 2 (X direction) shown in Figure 9**.**

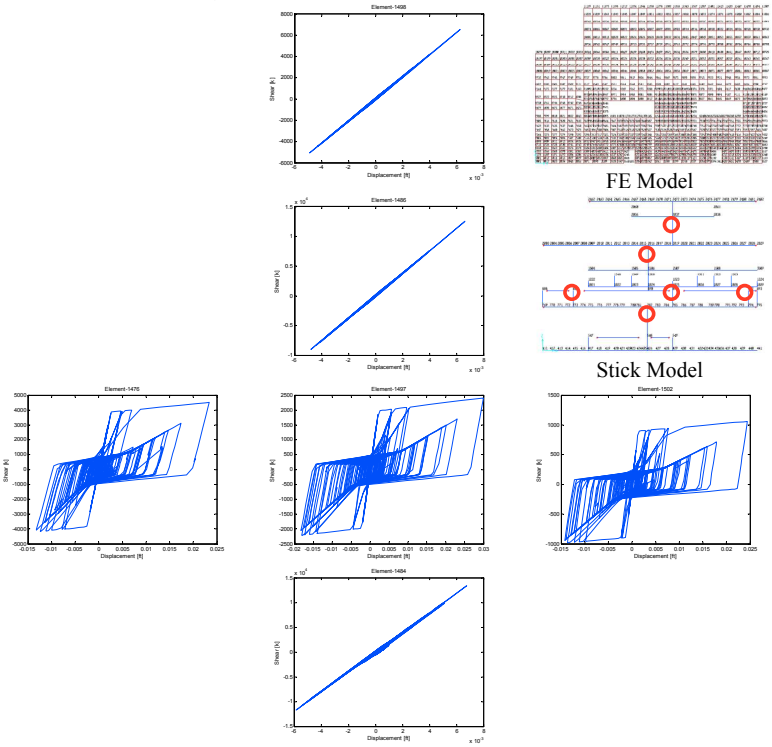

Figure 9. Example of the Nonlinear Shear Wall Response (16th realization of the HF motion, 1E-6 intensity level on the rock site – Column Line 2, X Direction)

In the ISSFA analysis of the subject structure, the structural failure is defined in terms of the interstory drift ratio (differential displacement between the top and bottom of each story divided by the height of that story). These drift ratios are calculated both in linear analyses and nonlinear analyses at each

input motion intensity level and for each LHS realization. Note that the linear analysis results represent the simplified (empirical) approach where the linear and nonlinear displacements during a seismic event are assumed to be equal. These results provide the drift ratio demand distribution at different ground motion intensity levels (input motion hazard level) which are used to construct the shear wall fragility functions. The maximum absolute interstory drift ratios (between the 1st and 2nd floors in the X direction) and the total drift ratios (differential displacement between the roof and base mat divided by the building height) for the building are presented in Figure 10 and Figure 11 for the subject structure supported on soil and rock subgrades, respectively. The drift ratios (in percentage) corresponding to the linear and nonlinear response for each LHS realization at each intensity level are shown by circular or triangular markers and their corresponding log-normal probability distribution functions are shown by the red and blue curves, respectively.

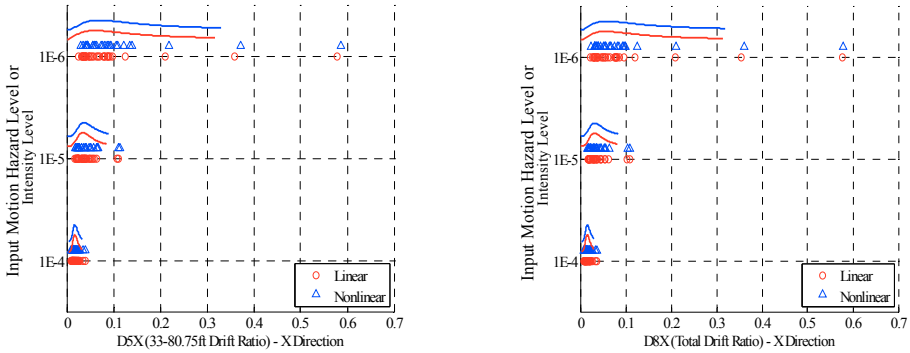

(a) 2nd Floor Interstory Drift (b) Total Drift

Figure 10. Comparison of Linear and Nonlinear Drift Ratios (in percentage), Soil Site, X Direction

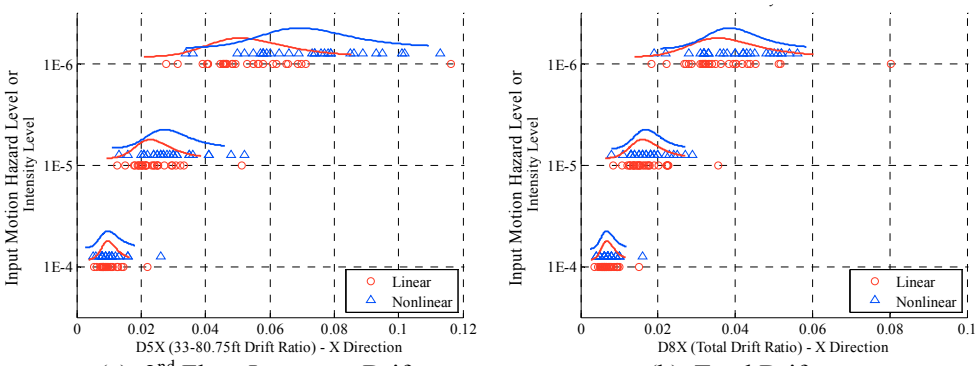

(a) 2nd Floor Interstory Drift (b) Total Drift

Figure 11. Comparison of Linear and Nonlinear Drift Ratios (in percentage), Rock Site, X Direction

6. CONCLUSION

Important observations from the nonlinear analysis of the subject structure including the SSI effects are summarized below:

- The probabilistic implementation of explicit structural nonlinearity in combination with the SSI effects are demonstrated using nonlinear response history analyses (RHA) of the structure with total foundation motions obtained from elastic SSI analyses, which are applied as input to fixed base inelastic analyses. This approach quantifies the expected structural nonlinearity for the particular structural configuration and selected demands parameters both at the design level and beyond design level seismic input. It also provides a robust analytical basis for the estimation of the changes in the probabilistic distribution of the structural demand parameters

due to structural nonlinearity.

- The ratio of the nonlinear to linear total drift for the shear wall structures can be reasonably taken as unity. This corroborates the widely used assumption that the linear and nonlinear total displacements are equal. However, locally, the nonlinear drift ratios may be significantly larger than the linear drift ratios due to concentration of the shear wall deformations at a single (weak story) level. Only a nonlinear analysis can account for such drift concentrations.

- The nonlinear analysis of the structure supported on soil and rock subgrades showed more significant evidence of structural nonlinearity in the case of the structure supported on rock. This is despite the fact that the total displacements observed in the soil case are more than twice those of the rock case. The reason is that the horizontal displacements calculated in the structure supported on soil are mainly due to the foundation rocking and soil deformations rather than the structural deformations even at beyond design intensity levels 1E5 and 1E6. This suggests that when the structure is supported on soil subgrade the SSI effects (including soil nonlinearity) are much more dominant than the structural nonlinearity effects.

- For both soil and rock supported structures the drift ratios calculated at design and beyond design levels are much smaller than the specified drift ratio capacity of the shear walls (estimated as 0.5% on average). This reflects the robustness of the structure and is typical of this type of construction for nuclear buildings where a larger component of the overall failure risk is due to non-structural components and equipment rather than the structural components. The fragility calculation and performance of such non-structural components and equipment are provided as part of the ISSFA analysis and will be discussed in future publications.

AKCNOWLEDGEMENT

The funding for this report was provided by Bechtel's Technical Excellence Program through the 2011 Full Technical Grant award. Throughout the development of this work, the advice and expertise of many of our colleagues was used. Without their help and support the fulfillment of this work would have been impossible.

REFERENCES

American Society of Civil Engineers (2007). Seismic Rehabilitation of Existing Buildings (ASCE 41-06 and Supplement-1), ASCE, Reston, Virginia, USA.

American Society of Civil Engineers (2005). Seismic Design Criteria for Structures, Systems, and Components in Nuclear Facilities (ASCE 43-05), ASCE, Reston, Virginia, USA.

Elkhoraibi, T.E. and Hashemi, A. (2011). Integrated Soil-Structure Fragility Analysis Method for Nuclear Structures. *Fifth International Conference on Earthquake Geotechnical Engineering*. Santiago, Chile, 10–13 January 2011.

Elkhoraibi TE and Hashemi, A. (2012). Design Applications for Integrated Soil-Structure Fragility Analysis. Bechtel Technical Grant Report.

Hashemi, A. and Elkhoraibi, T.E. (2009). Integrated Soil-Structure Fragility Analysis Method. *ECCOMAS Thematic Conference on Computational Methods in Structural Dynamics and Earthquake Engineering [COMPDYN 2009]*, Rhodes, Greece, 22–24 June 2009.

Hashemi, A., Elkhoraibi, T.E., and Ostadan, F. (2011). Probabilistic and Deterministic Soil Structure Interaction (SSI) Analysis. *Eleventh International Conference on Application of Statistics and Probability in Civil Engineering (ICASP11)*, ETH Zurich, Switzerland, 1–4 August 2011.

Mazzoni, S., McKenna, F., Scott, M.H., Fenves, G.L., et al. (2006). Open System for Earthquake Engineering Simulation User Command-Language Manual. Pacific Earthquake Engineering Research Center, University of California, Berkeley, OpenSees version 1.7.3.

Bechtel (2011). SASSI2010 - A System for Analysis of Soil-Structure Interaction. Bechtel Standard Computer Program (SCP), GE996 Version 1.0., November 2011.

McKay, M.D., Beckman, R.J., and Conover, W.J. (1979). A Comparison of Three Methods for Selecting Values of Input Variables in the Analysis of Output from a Computer Code. *Technometrics*, **21:2**, 239-245.

Wang, T.Y., Bertero, V.V., and Popov, E.P. (1975). Hysteretic Behavior of Reinforced Concrete Frame Walls. Earthquake Engineering Research Center (EERC), Report No. 75-23.